

CRISPR-Cas9 mediated xylose auxotrophy in *Scheffersomyces stipitis*

By

Samuel Johnson

A Thesis Submitted in Partial Fulfillment

Of the Requirements for the Degree of

Master of Science in Biology

Middle Tennessee State University

March 2024

Thesis Committee:

Dr. Brian Robertson, Chair

Dr. David Nelson

Dr. Matthew Elrod-Erickson

ABSTRACT

Scheffersomyces stipitis is a top xylose fermenter. The yeast efficiently ferments xylose into ethanol, making it industrially important. In this study, I (1) create a new toolset to knock out and replace any gene in the *S. stipitis* genome and (2) show the phenotypic alterations in the yeast's xylose fermentation after knocking out the *HXK1* gene which encodes *HXK1*. This experiment compares sugar utilization in wild-type and *HXK1* knockout strains. The unique toolset BLINCAR (Bioluminescent Indicator Nullified by Cas9 Actuated Recombination) demonstrated that I could knock out *HXK1* in *S. stipitis*. I tested this utilizing molecular and yeast biotechnology. The results reveal that *HXK1* knockouts utilize glucose similarly to the wild type. Since knocking out *HXK1* does not cause xylose auxotrophy, other glucose phosphorylation enzymes might be responsible.

TABLE OF CONTENTS

List of Figures	iv
List of Tables	v
CHAPTER 1: INTRODUCTION.....	1
Chapter 1.1: Biofuels	1
Chapter 1.2: Xylose.....	4
Chapter 1.3: <i>Scheffersomyces stipitis</i> and sugar metabolism.....	5
Chapter 1.4: Bioluminescence and Bioluminescent reporters	7
Chapter 1.5: BLINCAR	8
Chapter 1.6: CRISPR/Cas9.....	9
Chapter 1.7: Homologous Recombination.....	11
Chapter 1.8: Main Approach, Objectives and Question.....	13
CHAPTER 2: RESEARCH INVESTIGATION	14
Chapter 2.1: Results and discussion.....	14
Chapter 2.2: Materials and methods	33
Chapter 2.3: Conclusion.....	41

List of Figures

Figure 1: Luciferase reaction	7
Figure 2: Cas9 Enzyme	10
Figure 3: Homologous Recombination	12
Figure 4: <i>HXK1</i> Homology Arms	16
Figure 5: PCR amplified <i>HXK1</i> Homology Arms	17
Figure 6: PCR Screen of Homology Arms in pWR95	19
Figure 7: Plasmid orientation PCR Tests.....	20
Figure 8: Complete plasmid orientation PCR test	21
Figure 9: Complete blink in plasmid illustration	22
Figure 10: Blink in procedure diagram.....	23
Figure 11: Image of bioluminescing colonies.....	24
Figure 12a: Blink in PCR test diagram.....	25
Figure 12b: Blink in gel electrophoresis results	25
Figure 13: Diagram of blink out plasmid.....	26
Figure 14: Diagram of blink out procedure	27
Figure 15: Diagram of the CAR scar formation	27
Figure 16: Photograph of non-bioluminescent colonies	29
Figure 17a: Blink out PCR test diagram.....	29
Figure 17b: Blink out gel electrophoresis results	29
Figure 18a: Mutant HPLC data results	31
Figure 18b: Wild type HPLC data results.....	31

List of Tables

Table 1: qRT-PCR data results	33
Table 2: Table of Primers	33

Chapter 1 Introduction

1.1 Biofuels

The term *green biotechnology* broadly describes the application of molecular techniques to engineer life for the purposes of advancing agricultural development and promoting sustainability (Barcelos *et al*, 2018). The objective of agricultural development seeks to produce drought-resistant and pest-resistant genetically modified plants for human benefit as well as biotransformation and plant-derived biopolymer production. Sustainability encompasses the initiative for technologies that serve to repurpose feedstocks into renewable energy and also seeks to offset carbon dioxide produced by fossil fuel utilization. One way that feedstocks (and feedstock wastes) are used is via the production of biofuels.

Biofuels offer a more expeditious fuel source in comparison to fossil fuels, which necessitate extensive geological time spans for their formation. Fossil fuels, in their most rudimentary sense, have existed for eons in the form of coal (Qiu *et al*, 2023). Biofuels refer to a category of fuels derived from biomass within a relatively brief timeframe, as opposed to the protracted process of fossil fuel generation. Biofuel use started in the early nineteenth century with the invention of an ethanol powered engine (Morey, 1826). Biofuels have since gained in popularity because often only sunlight and water are needed to generate biomass, which can then be converted into fuel. This makes biofuels a renewable energy source. Biofuels have received more recent attention lately because of the global effort to reduce carbon emissions. There is now a push to include biofuel production in the United States so that the country is less dependent on imported fossil

fuels from OPEC countries (Charles, *et al*, 2007). Biofuels can be divided into three categories – first, second and third generation based on the amount of biochemical complexity and feedstock development streams needed to produce the fuel (Lee *et al*, 2013).

First-generation biofuels refers to the fermentation of mainly edible feedstocks, high in glucose and other easily accessible 6-carbon sugars (Lee, *et al*, 2013). Examples of this include fermenting sugarcane effluent and malted corn grain directly into ethanol. Another example of a first-generation biofuel is vegetable oil conversion into biodiesel. Currently most of the United States’ production of biofuel is first-generation. Ethanol is the largest source of biofuel (85 percent) (U.S. Energy Information Administration, 2022). Currently around 45 percent of all corn crops are dedicated to ethanol production (U.S. Department of Agriculture, 2022). First generation biofuels offer several advantages that have contributed to their widespread use. Advantages of first-generation biofuels are that they are renewable; they reduce greenhouse gases, and they absorb carbon dioxide from the atmosphere. The disadvantages of first-generation biofuels include cropland over-use, competition with food crops (the food vs fuel debate) and in some cases the energy output may not be higher than the energy input, raising questions about overall efficiency (United States Environmental Protection Agency, 2023).

Because of these disadvantages, research and industry leaders are exploring biofuel production streams that produce fuels from other feedstocks besides food-related ones.

Second-generation biofuels utilize lignocellulosic feedstocks and agricultural wastes. Examples of this include fermenting corn cob (which is rich in xylan) into ethanol, and fermenting wood cellulose and hemicellulose into ethanol (Gandam, *et al*,

2022). There are many possible kinds of second-generation biofuel feedstocks. Corn stover, sawdust from sawmills, wheat chaff, grass clippings, are a few of the feedstocks used in cellulosic ethanol production. Currently, most of these materials are composted or allowed to biodegrade which just renders their high energy carbon down to CO₂. Second generation production streams try to capture this high energy carbon from these “waste” materials for a usable purpose before it is converted to CO₂.

The advantages of second-generation biofuels include no competition for food agriculture, a rich and diverse stream of other high energy carbon sources in addition to glucose, and their utility as a waste management solution (Kowalski, *et al*, 2022).

However, the drawbacks include the inaccessibility of fermentable carbon from these sources [cellulose, hemicellulose, lignin], the high cost of liberating these carbon stores, the biochemical inhibitors that are released/produced during lignocellulosic preprocessing and fermentation, and the diverse processing streams that are required for the complexity of different fermentable sugars. All of these barriers add costs and reduce efficiency. Because the potential advantages of second-generation biofuels are so high, it is worth investing research and resources toward mitigating the costs and disadvantages of the current state second-generation biofuel production. One such avenue is to increase the fermentation efficiency of secondary sugars, such as xylose, that are liberated from processed lignocellulosic biomass.

1.2 Xylose

Cellulose, hemicellulose, lignin, and pectin are the principal structural components of vascular plants (Cruz, *et al*, 2014). The ratio of these materials determines the form of vascular plants. For example, flexible, leafy material is often higher in cellulose; dense woody material is often higher in lignin and hemicellulose; and fruity, floral material is often higher in pectin (Gibson, 2012). Hemicellulose is composed of xylose monosaccharides in addition to other monosaccharides like glucose, mannose, arabinose, or galactose (Bajpai, 2018). Xylose is a pentose sugar that adds rigidity to the uniform crystalline polysaccharides present in vascular plant tissue (Rennie, 2014). Hemicellulose is broken down into xylose via pretreatment at biorefineries.

Xylose, however, has only recently been investigated as a source of bioethanol. The five-carbon sugar is the second-most abundant renewable carbon source beneath glucose (Mellerowicz and Gorshkova, 2011). If xylose could more economically be converted into ethanol, it could greatly increase ethanol yield from biomass. The problem is, the majority of first-generation biofuels and glucose fermentation is performed by *Saccharomyces cerevisiae*, a yeast that is highly efficient, widely studied and is extremely easy to genetically engineer and manipulate. However, *S. cerevisiae*'s ability to ferment the variety of other sugars liberated from hemicellulose (including xylose) ranges from absent to poor (Ruchala, *et al*, 2020). Contemporary studies have identified *Spathospora passalidarum* (*S. passalidarum*) and the closely related *Scheffersomyces stipitis* (*S. stipitis*) as the best yeasts in fermenting xylose into ethanol (Hou, 2011), so research involving this non-mainstream yeast may provide strategies for improving the efficiency of second-generation biofuel production.

1.3 *Scheffersomyces stipitis* and sugar metabolism

S. stipitis is a haploid yeast that lives in the guts of passalid beetles. This endosymbiont allows the beetle to digest recalcitrant hemicellulose and its constituent xylose. *S. stipitis* has coevolved with the beetle to be excellent at fermenting xylose (Suh, *et al*, 2005). The beetles burrow deep into the wood of softwood trees using the microbial symbiont to consume numerous types of hemicelluloses (Suh, *et al*, 2003).

In *S. stipitis*, glucose is imported into the cell by a hexose transporter. Once it is in the cytosol, glucose is modified by the enzyme, hexokinase, which phosphorylates glucose (at the sixth carbon) preventing the hexose sugar from diffusing back outside of the cell. This phosphorylation step is the first step of glycolysis, and interfering with it will alter the way that glucose is metabolized. Typically, this means that the yeast will divert its metabolism into utilizing other sources of carbon (Nilsson, *et al*, 2016). In nature, or in a mixed sugar medium, wild type *S. stipitis*, like many microbes, will consume glucose first, disregarding other sugars, until glucose is depleted. This is an evolved metabolic strategy called diauxic growth that allows the microbe to preferentially process the higher energy-yielding glucose first, before processing other sugars, which yield less energy from their catabolism. If *S. stipitis* could be genetically modified so they are forced to solely ferment xylose regardless of whether glucose was present or not, the mutant *S. stipitis* could serve as a keystone organism in the production of advanced (second-generation) biofuel.

Prior studies in wild type *S. stipitis* have shown that deletion or interruption of the gene, *HXK1*, which encodes for the key glycolysis enzyme *HXK1*, can lead to altered glucose and xylose metabolism (Dashtban, *et al*, 2015). When researchers deleted the

hexokinase gene, there was a slight difference in the way that wild type and the knockout mutant processed xylose. For the last hour of glucose fermentation, of a xylose-glucose mixture, the xylose was consumed at the same time as the glucose. This study only focused on knocking out the *HXK1* gene so it stands to reason that knocking out *HXK1* isoforms could further mitigate the diauxic restrictions to xylose utilization.

Bioinformatics predicts that *S. stipitis* has four hexokinase isoform genes: *HXK1*, *GLK1* (glucokinase 1), *GLK2* (glucokinase 2) and *NAG5* (N-Acetylglucosamine Kinase). One would expect that in order to eliminate glucose phosphorylation, one would have to disrupt each of these four genes, otherwise any of the remaining gene products could compensate for the loss of any others. As of yet, there have been no studies that eliminate all four hexokinases. One barrier for such a four-fold gene deletion is the limited set of selectable markers and molecular tools developed for *S. stipitis*. About a decade ago, the Robertson lab started developing biotechnology tools for *S. stipitis*. The yeast was just beginning to gain attention in the biofuels industry because of its ability to ferment xylose into ethanol. *S. stipitis* is in the CUG clade, a group of yeasts in which the codon CUG encodes for serine instead of leucine (Santos, *et al*, 1995). Many yeasts in the CUG clade were barely characterized. Since then, the Robertson lab has engineered a myriad of codon optimized coding sequences, selection markers, and recombination elements—all of which have developed into a recently published toolset for *S. stipitis*, the BLINCAR system, which allows for on-demand addition or removal of genes in *S. stipitis* (Reichard, *et al*, 2023). BLINCAR employs a novel gene modification technique that replaces a targeted, yeast genomic DNA sequence(s) with an antibiotic-selectable bioluminescent reporter construct. Successfully targeted, glowing, transformants are then

liberated of both the targeted genomic DNA and the bioluminescent reporter construct to allow subsequent re-uses of the technology to remove other DNA sequences of interest (Reichard, *et al.*, 2023).

1.4 Bioluminescence and Bioluminescent Reporters

Pyrophorus, a type of click beetle, incorporate bioluminescence into all parts of their life cycle. They bioluminesce when they are eggs and glow as larvae. At adulthood, they have two pronounced bioluminescent pronotum spots and an inner bright light organ that is brighter than the pronotum spots (Harvey, *et al.*, 1928; Levy, 2008).

Bioluminescence occurs when luciferase is catalyzed with luciferin and ATP molecules and oxygen and magnesium. The emission of light is caused by formation of a product (or intermediate) when it is in an electronically excited state. Returning to the ground state occurs through a light photon (Baldwin, 1996).

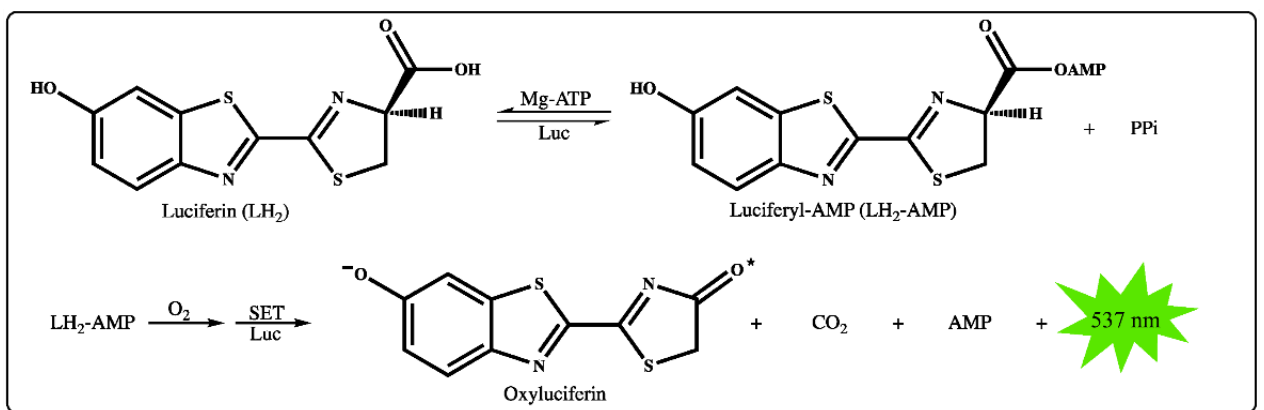


Figure 1, The mechanism of luciferase

Figure 1 above, (modified from Branchini, *et al.*, 2022) illustrates the mechanism of luciferase-catalyzed bioluminescence in *Pyrophorus* click beetles. Luciferin is

oxidized and converted into oxyluciferin releasing green light at 537nm (Miloud, *et al*, 2007; Mezzanotte, 2011).

The genetic code for the *Pyrophorus* beetle luciferase has been used for decades in a myriad of applications including yeast biotechnology. One of the most common uses for luciferase encoding genes, including the ones from *Pyrophorus*, are as reporter genes. In these applications, the light given off as a result of the protein's production, activity, and color inform researchers about certain occurrences happening within the cell, such as gene regulation, oxygen abundance, sugar utilization, and pH changes (Robertson, *et al.*, 2008; Krishnamoorthy and Robertson, 2015; Zhang, *et al.*, 2012).

When a bioluminescent reporter gene, such as CBG99 from *Pyrophorus*, is fused into the gene replacement element of a gene-deletion technology, the gene is transcribed and translated to protein, and its resulting bioluminescence can be a useful reporter for identifying potential genomic alterations of yeast grown on solid media containing the luciferin substrate.

1.5 BLINCAR

The technique named, BLINCAR (Bioluminescent Indicator Nullified by Cas9 Actuated Recombination), refers to a two-part technology for genomic alteration. The first part involves an insertable genetic element for *S. stipitis* that provides a selectable, bioluminescent phenotype for cells that integrates that element when replacing the gene to be deleted by homologous recombination (Reichard, *et al*, 2023). This results in a simultaneous deletion of target DNA and replacement with the element. Once targeting and gene deletion has been confirmed in the strain by PCR, the portion of the integrated

construct bearing the bioluminescent protein encoding gene, coCBG99 (Codon-Optimized Click Beetle Green) and the antibiotic resistance gene can then be removed by cutting and recombining the genomic DNA at the CAR (Cas Actuated Recombination) sites by introducing the second part of this technology, a plasmid that encodes a sgRNA and Cas9 (Reichard, *et al*, 2023). Henceforth the two steps of the BLINCAR technique will be referred to as “blink in” and “blink out.” In addition to bioluminescence and antibiotic selection, the BLINCAR system makes use of CRISPR-Cas9 gene editing and yeast’s natural ability to perform homologous recombination, topics that are elaborated below.

1.6 CRISPR-Cas9 Gene Editing

CRISPR-Cas9 gene editing is a molecular biology technique that can change the DNA of living things *in vivo*. This system is based off of the natural defense mechanisms of bacteria and archaea against reinfection from exogenous DNA (Jinek, *et al*, 2012). CRISPR stands for clustered regularly interspaced short palindromic repeats. These are pieces of plasmid or viral DNA that are sequestered away in the bacterium’s genome for later transcription into RNAs used for fighting off reinfection. This sequence of RNA that identifies viral DNA is referred to as the crRNA (CRISPR RNA). The CRISPR system uses Cas endonucleases such as Cas 9 to search for and cut the DNA sequence complementary to the crRNA (Jinek, *et al*, 2012). Specifically, the Cas9 enzyme cuts three nucleotides upstream of the Protospacer Adjacent Motif (PAM) sequence, generating a double stranded break (DSB) in the DNA of an infecting virus (Figure 2).

Researchers have reverse engineered the CRISPR-Cas9 system for use in targeted host cells by providing them a source of Cas9 protein and a synthetic guide RNA (sgRNA) in place of the crRNA, and in so doing coopted the system to make targeted cuts to genomic DNA by controlling which sgRNAs are expressed in the presence of the encoded Cas9. After which, the processes of non-homologous end joining (NHEJ) and homologous recombination (HR), which will be discussed in detail later, are the primary ways that these DSBs are repaired when genomic DNA is cut.

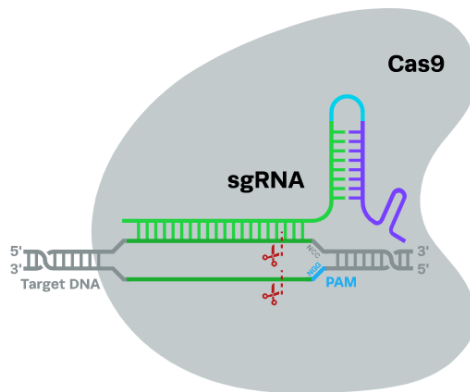


Figure 2, The Cas 9 enzyme creates a double stranded DNA break three base pairs upstream of the PAM sequence.

Evolution has produced three types of naturally occurring CRISPR-Cas systems that have been characterized: type I, type II, and type III (Makarova, *et al*, 2015). Each system is distinguished by unique genes: Cas3 in type I, Cas9 in type II, and Cas10 in system type III. (Makarova, *et al*, 2015). BLINCAR uses a type II CRISPR-Cas system. A type II CRISPR-Cas system consists of an effector module comprised of a solitary,

multidomain protein (Chylinski, *et al*, 2014) as opposed to the other systems whose endonuclease activity is the product of several proteins working together. When implementing CRISPR-Cas systems in non-native cells, type II systems are easier to deliver since they require only a couple of exogenous parts, a gene that encodes the Cas9 endonuclease, and a genetic element that codes for sgRNA production. BLINCAR uses Cas9 to liberate the yeast cell of its bioluminescent marker and antibiotic selection construct by generating DSBs on both sides of this transgenic element. After these cuts are made, the cell uses its own homologous recombination machinery to accurately repair the DSB.

1.7 Homologous Recombination

Homologous recombination (HR) refers to the template-dependent repair of double stranded DNA breaks. This process protects the genetic integrity of all three domains of life (Li and Heyer, 2008). HR serves the purposes of nucleotide repair and recombination. HR begins with the recognition of DNA damage. The broken DNA ends are processed (in Fig. 3) to generate single stranded DNA (ssDNA) tails. These single stranded tails eventually pair with a homologous DNA template. These tails search for a homologous region on an intact DNA molecule, which usually comes in the form of a sister chromatid, homologous chromosome, or provided homology template (Li and Heyer, 2008). After this the ssDNA forms a structure called a displacement loop (D-loop) by invading the intact DNA molecule and base-pairing with a complementary sequence (Krejci, *et al* 2012). Sometimes DNA strands are swapped between broken and intact molecules which results in the repair of the damaged DNA. After this comes branch

migration, which involves the movement of a DNA strand within a DNA molecule in the context of recombination intermediates called Holliday junctions (Constantinou, *et al*, 2001). After this the D-loop is resolved and the repaired DNA molecule is separated from the template.

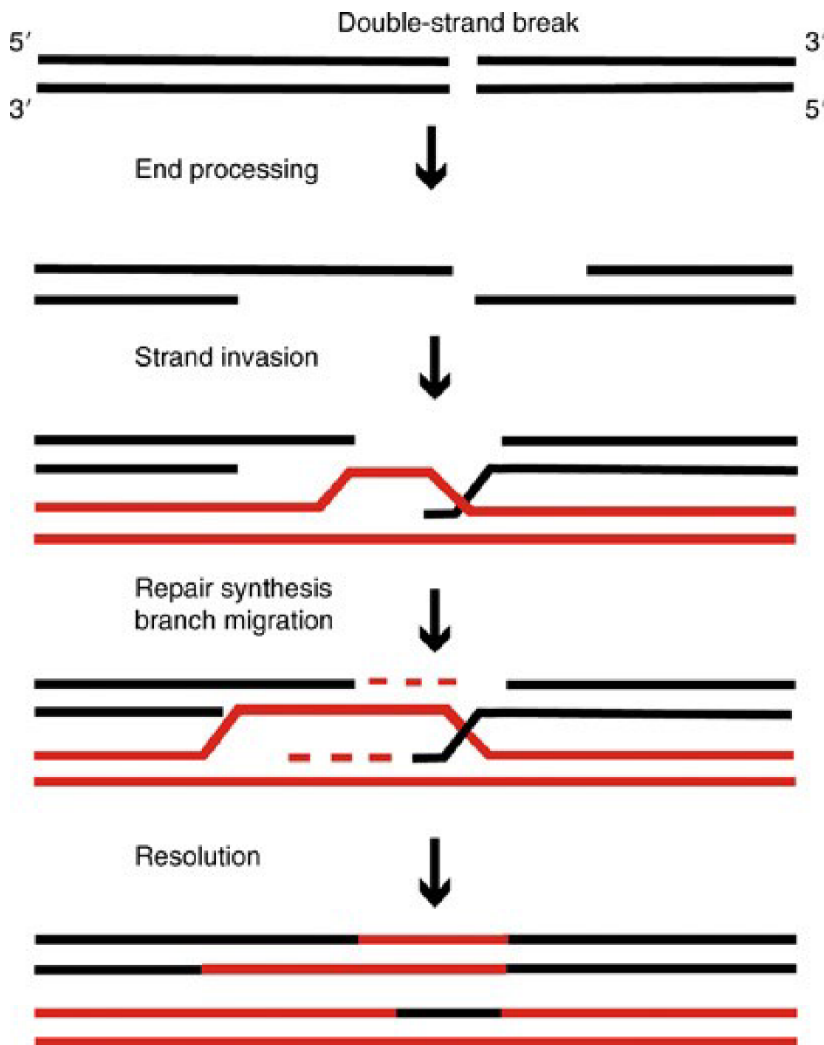


Figure 3, Homologous Recombination modified from Thacker J in the Encyclopedia of Cancer. The broken DNA molecule (black) is processed to give long single stranded regions that invade an undamaged homologous molecule (red). The branched-out undamaged strand guides break repair. With repair synthesis (red dashes) comes branch migration. Resolution cuts the connections between the molecules without crossing-over.

Homologous recombination is a high-fidelity DNA repair mechanism because it relies on a homologous DNA template. Homologous recombination is essential during meiosis to generate genomic diversity by transacting nucleotides between homologous chromosomes. It also plays a role in non-meiotic cells to repair DNA if broken.

BLINCAR uses homologous recombination to genetically manipulate yeast strains, first by introducing into the host genome a piece of exogenously provided DNA containing the bioluminescence and antibiotic resistance encoding genes flanked by portions of homology to the genomic region of the host cell to be targeted, then again later when an effector plasmid expressing Cas9 facilitates the deletion of the bioluminescent and antibiotic resistance markers.

1.8 Main Approach, Objectives, and Question:

This project aimed to use BLINCAR to remove the *HXK1* gene from *S. stipitis* and then characterize the phenotypic effects of its gene loss on the yeast's ability to metabolize glucose and xylose. The hypothesis was that by deleting *HXK1*, *S. stipitis* would alter its metabolism of glucose in favor of xylose when grown on a mixed sugar. A secondary hypothesis is that by using BLINCAR to make this gene deletion, antibiotic sensitivity in the *HXK1*-deleted strain would be restored so that a subsequent gene deletion (of a different gene) could be made later using the same antibiotic. This aim was accomplished, and hypothesis tested by achieving the four targeted objectives below.

Objective (1) Plan and construct the BLINCAR elements to target *HXK1* for deletion.

Objective (2) Blink in the BLINCAR element to replace the target sequence.

Objective (3) Blink out the BLINCAR element from Objective (2) to restore sensitivity to the selection antibiotic.

Objective (4) Compare sugar usage of the mutant yeast versus wild type *S. stipitis* using HPLC and qRT-PCR.

Chapter 2 Results and Discussion

Introduction

In this section I present the results of my study and engage in a comprehensive discussion of their implications. I subdivide the results and discussions based on the four objectives mentioned in Chapter 1. First, in objective 1, I adapt the BLINCAR system for replacing *HXK1* by targeting upstream and downstream homologies. After this, in objective 2, I fulfill the previous objective via using homologous recombination to replace *HXK1* with the antibiotic and bioluminescent genes as well as other sequences used during the blink out phase. In objective 3, I removed the element using a Cas9 enzyme that targets a sequence found nowhere in *S. stipitis* genome other than flanking the bioluminescence and antibiotic resistance genes of the introduced transgenic element. Antibiotic sensitivity was restored and only a scar remains in place of the element. The fourth objective involves a fermentation experiment in which the wild type yeast and the *HXK1* knockout yeast are compared for their ability to coferment xylose and glucose. Briefly, my findings reveal that there is no noticeable difference in the way that the wild type versus the mutant utilizes a mixed media of xylose and glucose, that is to say that the

results did not support our initial hypothesis. This implies that secondary hexokinases are also responsible for glucose phosphorylation. This prompted me to perform a follow-up qRT-PCR experiment of *S. stipitis* growing on sugar to examine which kinase genes were being expressed.

Objective (1), Planning, designing, and building the BLINCAR system to replace *HXK1*:

BLINCAR allows one to target a genomic DNA sequence and swap it for an element that encodes for bioluminescent luciferase and antibiotic resistance proteins in *S. stipitis*, after which the element can be excised leaving only a small scar of the originally inserted element. The Robertson Lab had previously designed a repertoire of plasmids required for BLINCAR (see Reichard *et al.*, 2023), but for my work, I primarily just needed two of the published plasmids to achieve my objectives, namely pWR95 (the plasmid that contains “coCBG” the codon-optimized click beetle luciferase gene in tandem with “coKanMX” the codon-optimized G418 antibiotic resistance gene), and pWR63(*YUMI*), the plasmid that encodes Cas9, which targets the artificial *YUMI* sequences found in pWR95.

Prior work had experimentally determined that around 2,000 base pairs of flanking sequence were adequate to achieve homologous recombination which is



Figure 4, A model showing the genomic *HXK1* homology arms flanking the hexokinase gene. US Homology regards approximately 1.7 kb upstream of the 1.5 kb *HXK1* coding sequence and DS Homology regards approximately 2.1 kb downstream. The homology arms are represented in the sky-blue regions. The navy region has the *HXK1* gene which is 1,449 bp

consistent with that described by others (Cao, *et al*, 2017), so I began by adding upstream and downstream regions of *HXK1* homology to pWR95.

In order to insert the homology arms into pWR95, I first use *S. stipitis* genomic DNA as a template in a PCR reaction to clone both homology arms. I chose arms that were roughly 2 kb. The upstream arm is 1,756 (1,768 with primer restriction enzyme sites) bp and the downstream arm is 2,106 bp (2,118 bp with primer restriction sites). I recovered gel excisions of these amplicons (Figure 5).

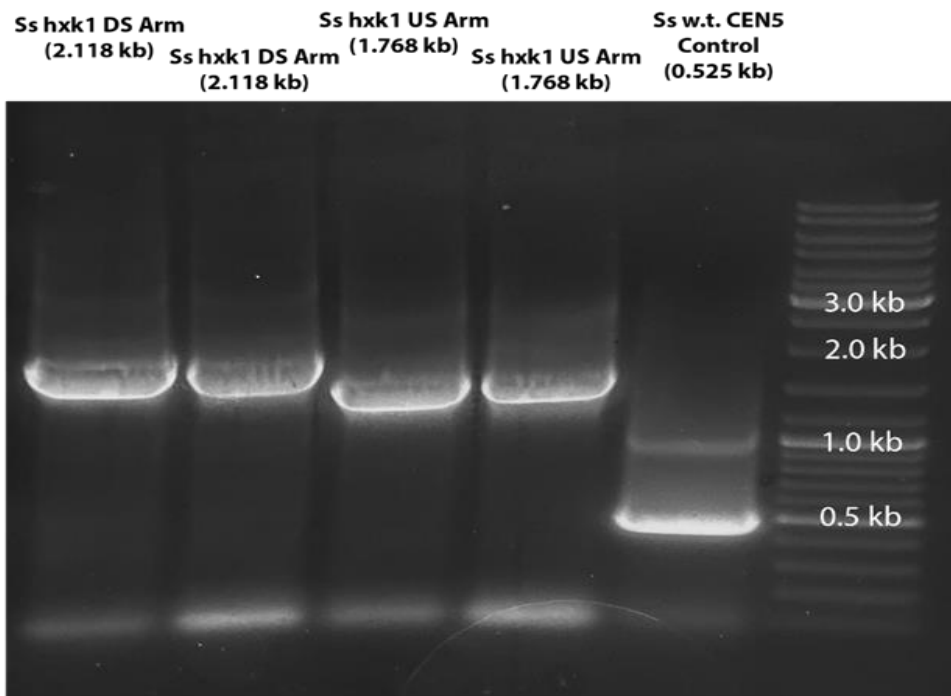


Figure 5, A gel that shows the homology arms that were amplified by PCR using wild type *S. stipitis* genomic DNA as template. Products from upstream and downstream homology arm reactions were loaded in duplicate as indicated above each lane. CEN5 was used as a positive control for genomic amplification.

When I PCR amplified these arms, I used primers that allowed us to ligate the homology arms into pWR95 vectors. For the upstream homology arm and its pWR95 vector, I used *AgeI* and *XbaI* to digest the amplicon DNA and pWR95 vector and generate sticky end overhangs. For the downstream homology and its pWR95 vector, to generate sticky ends, I used *NdeI* and *SacII*. After sticky ends were generated, I ligated pWR95 plasmids with either upstream or downstream homology arms thereby producing plasmids called *HXX1-US-pWR95* and *HXX1-DS-pWR95* respectively. After ligation, I transformed the plasmids into Top10 *E. coli*. The PCR test below (Figure 6) shows that for three candidate transformants for each of the two transformations, the complete

homology arms and vector were successfully transformed into chemically competent *E. coli*. In Figure 6, the middle lane is the molecular ladder. On the left side (lanes 1-3) is the product of PCR amplification of the downstream arm taken from three successfully transformant *E. coli* colonies. The three lanes to the right are the result of upstream PCR amplicons based on the templates of successfully transformant *E. coli*.

To support the PCR evidence of successful plasmid construction and transformation, the *HXK1-US-pWR95* and *HXK1-DS-pWR95* plasmids were subjected to restriction analysis to ensure that the homology arms have been added. I used the restriction enzymes *AgeI* and *XbaI* to digest *HXK1-US-pWR95*. The 9.764 kb plasmid was divided into 8.014 kb and 1.750 kb fragments. The *HXK1-DS-pWR95* plasmid, 10.103 kb in length, was restriction digested by the enzymes *NdeI* and *SacII*. This yielded a 2.102 kb fragment and a 8.001 kb fragment. In both cases the fragments were exactly where I predicted from doing an *in silico* analysis. The result of the gel electrophoresis in Figure 7 shows that both homology arms are in each of their respective pWR95 vectors.

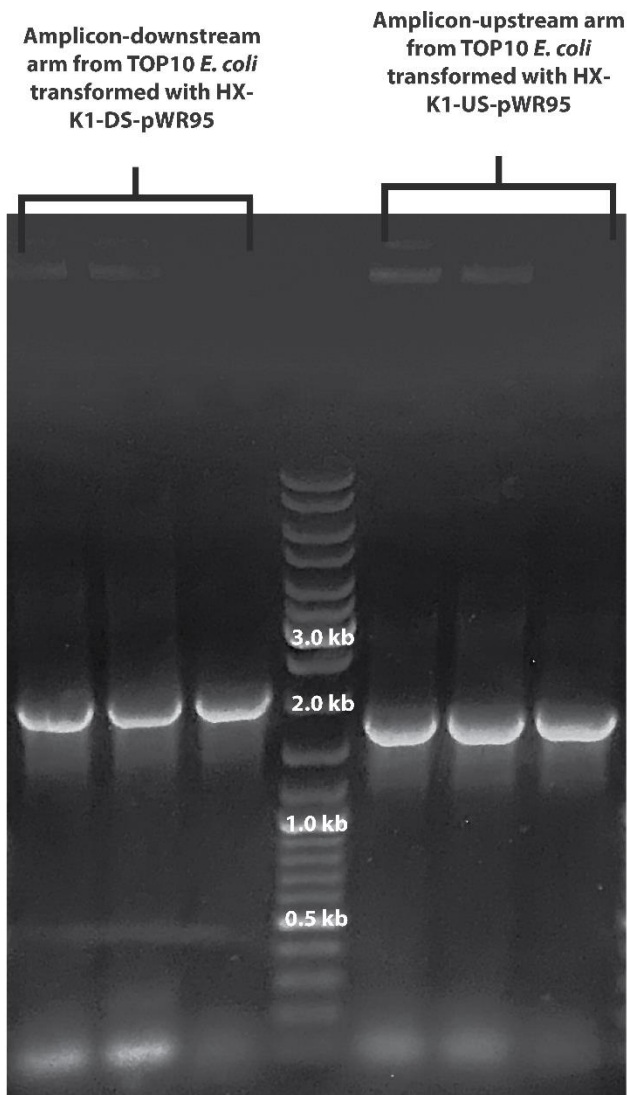


Figure 6, A colony PCR screen of E. coli transformants. After transformation and selection on Ampicillin, colonies were PCR screened for the template of the upstream and downstream homology arms.



Figure 7, A gel showing products of candidate plasmid digestion. I digested the two plasmids to ensure that they were in the correct orientation. Each plasmid broke up into two pieces that are compared to the molecular ladder in lane one.

Next, to assemble one plasmid that contained both homology arms, I cut *HXK1-US-pWR95* with *NdeI* and *SacII* to prepare it for receiving the downstream homology arm from *HXK1-DS-pWR95*, which was isolated by cutting it with *NdeI* and *SacII* as well. I ligated the downstream homology arm into the larger *HXK1-US-pWR95* linearized plasmid to produce the plasmid called *HXK1-USDS-pWR95* then transformed

the fully assembled plasmid into Top10 competent *E. coli*. After transformation, I tested that the arms were properly ligated into pWR95 via restriction enzyme digestion analysis. I used the enzyme *HindIII* to linearize the plasmid into two fragments. This yielded a 9,889 bp and an 1,885 bp fragment (Figure 8). These fragment sizes corresponded to those expected if constructed correctly. Had the downstream arm failed to ligate into the receiving vector, then only one *HindIII* site would have been present in the plasmid and therefore only one band would have been produced.

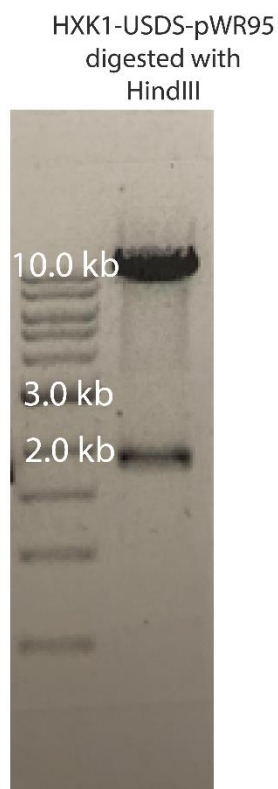


Figure 8, A gel showing HXK1-USDS-pWR95 digested with *HindIII* for confirmation of construction. The completed blink in plasmid cuts into a 9.889kb and a 1.885 kb set of fragments if constructed properly

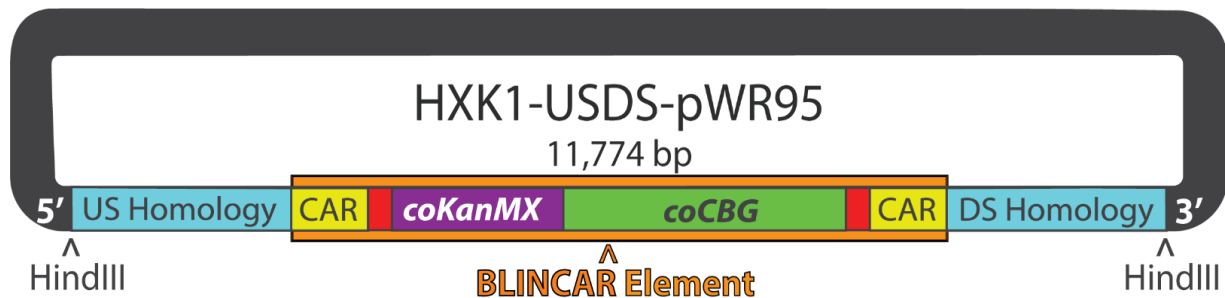


Figure 9, the pWR95 Blink In disruption plasmid with its elements and HXK1 homology arms. The Upstream (US) homology arm and Downstream (DS) homology arms flank the Cas actuated (CAR) sites. A codon optimized Geneticin selectable marker (coKanMX) and a bioluminescent reporter codon-optimized Click Beetle Green (coCBG) comprise the core of the element. Unlabeled in red are Cas9 targeting sites for excising the cassette during the blink out phase. HindIII sites flank the entire cassette so that HindIII can be used to linearize and isolate the functional portion of the plasmid from its *E. coli* replication and selection elements. Highlighted in orange is the BLINCAR element. It should be noted the features of this plasmid model are not drawn to scale. The portion between the HindIII sites that contains the BLINCAR element and homology regions is 9.889 kb, while the remaining gray portion is 1.885 kb.

After I confirmed correct assembly of the construct, *HXK1*-USDS-pWR95, I maxipreped the plasmid and then linearized it with *HindIII* to transform wild type *S. stipitis* with the resulting linearized fragments. Of the two fragments, the 9.889 kb disruption cassette contained the BLINCAR element and *HXK1* upstream and downstream homology regions, and it was this fragment that was designed to integrate and replace *HXK1*. The other fragment of the plasmid (approximately 1.9 kb) was expected to be innocuous to the *S. stipitis* transformation.

Objective (2), Blinking in the disruption element:

This objective of this part of the project involves the introduction of the BLINCAR cassette into wild type *S. stipitis*, replacing the native *HXK1* coding sequence. Here I chemically transformed *S. stipitis* with the linearized plasmid that replaces the genomic *HXK1* gene with a Geneticin (*coKanMx*) resistance marker and a codon optimized click-beetle-green-99 (*coCBG99*) gene (Figure 10). This simultaneously exchanges the *HXK1* gene with the BLINCAR element via homologous recombination (HR). The BLINCAR element is thus nested in between two homology arms within the *S. stipitis* genome. Successful transformants are luminescent in the presence of luciferin, can survive on Geneticin-containing media, and yield a positive genotype PCR test.

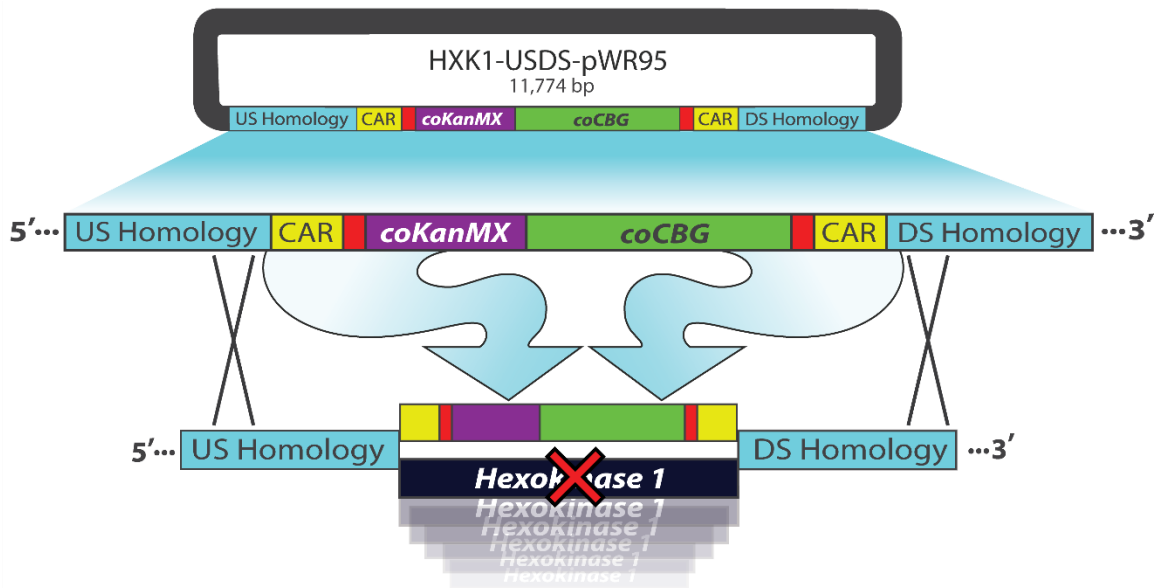


Figure 10, The linearized effector plasmid is transformed into wild type *S. stipitis*. The BLINCAR element replaces the *HXK1* gene via homologous recombination. The BLINCAR element is nested in between the genomic homology arms.

Geneticin is only partially effective as a selection agent for *S. stipitis* and it is common for background colonies to form on the second and third days of selection (Figure 11). However, the bioluminescent quality of transformed cells illuminated candidate colonies to pursue for further investigation.

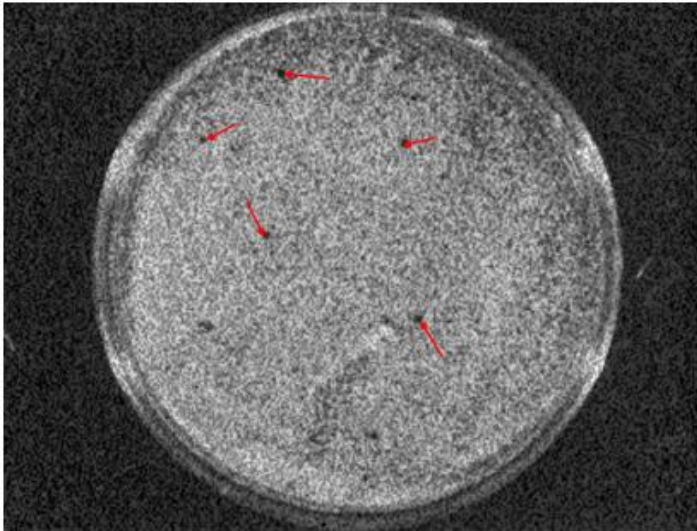


Figure 11, A photograph of bioluminescent *S. stipitis* colonies growing on agar containing Geneticin and luciferin. The picture consists of merged images comprising a brightfield image showing all colonies and an inverted bioluminescent image (5 min exposure) with bioluminescence showing up as black colonies. The colonies with red arrows are glowing. These colonies were subcultured, and PCR screened for proper integration of the BLINCAR element.

It was possible that some transformants exhibiting bioluminescence integrated the BLINCAR element into *S. stipitis* at an unintended site in the genome (somewhere off-target), so candidate transformants were PCR screened to confirm proper BLINCAR targeting to the *HXK1* locus. This was accomplished by making upstream and downstream PCR primers that amplify portions of the introduced disruption element and

the *S. stipitis* genome (Figures 12 a and b). Both PCR reactions yielded products at the expected length of 3.20 kb. This demonstrated that the BLINCAR element is indeed accurately present at the expected loci of the glowing yeast colony's genome.

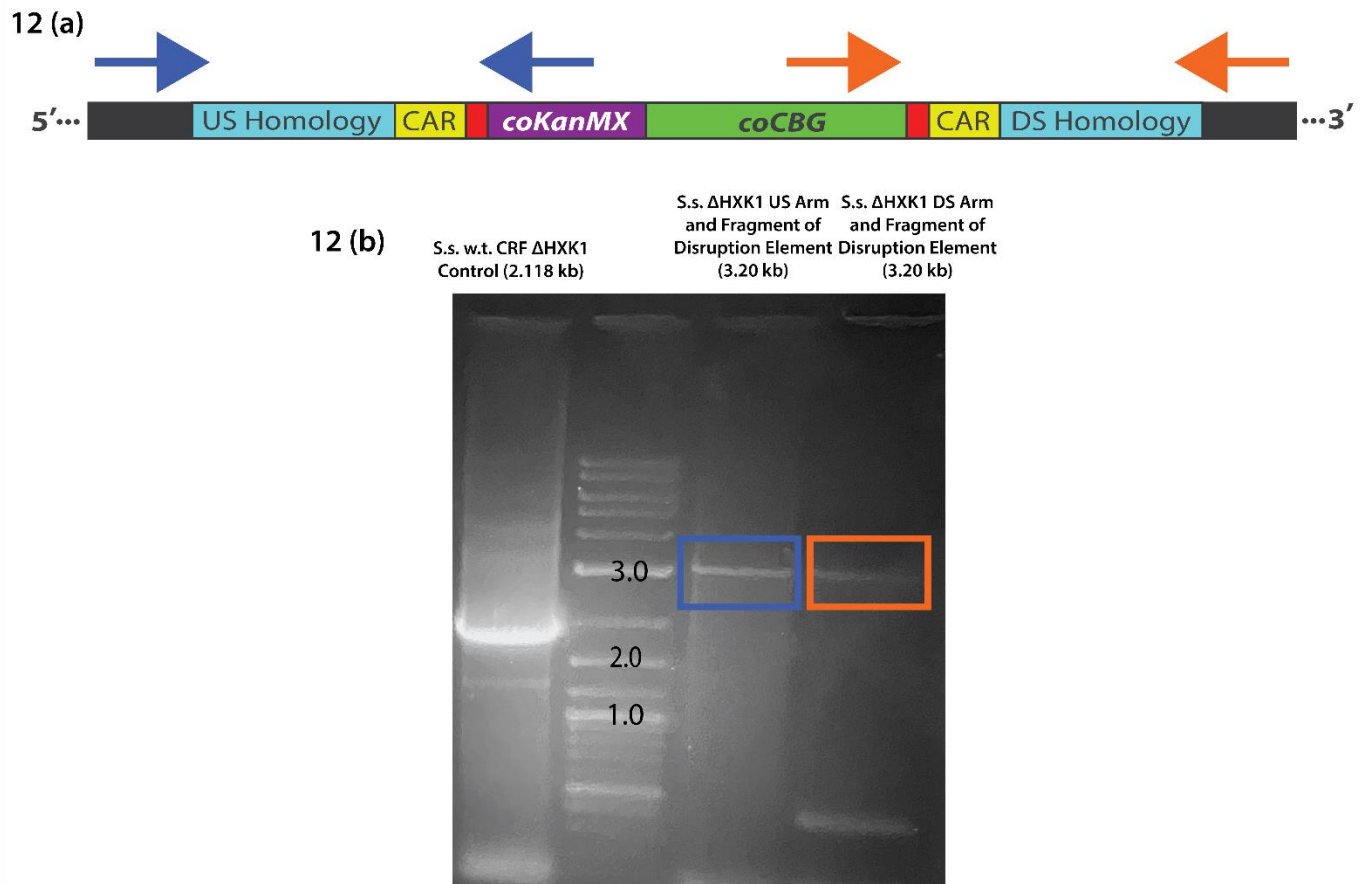


Figure 12 (a), I PCR amplified the brightly glowing colony's template DNA. The amplicons contain sequences derived from both genomic and artificial sequences. The blue arrows are primers for amplifying an upstream region from in the genome to the CoKanMX gene. The orange arrows are the primers for amplifying the downstream region in the genome to the coCBG99 gene. Figure 12 (b), demonstrates that not only has the element been integrated into the genome, but also, it is integrated into the genome correctly. Each box in the gel corresponds with the same color marked primers in 12 (a).

Objective (3), Blinking out the disruption element:

I next transformed successful knockouts from the blink in stage with the effector plasmid, pWR63(*YUMI*) (Figure 13). pWR63(*YUMI*) contains a segment of DNA that encodes a ctRNA that targets Cas9 to an artificial sequence *YUMI* in pWR95 that is otherwise absent from the *S. stipitis* genome (dark blue in figures 13 and 14). The plasmid also contains an accompanying Cas9 nuclease gene optimized to function in the CUG-clade yeast *Candida albicans* (Vyas *et al*, 2015) whose protein functions to excise the coKanMx resistance marker as well as the coCBG99 gene. The pWR63(*YUMI*) plasmid also contains a Codon Optimized Hygromycin (*coHPH*) resistance marker and a *S. stipitis* autonomously replicating sequence (*ARS*). Successful transformants for this second phase grow on plates containing Hygromycin and do not bioluminesce.

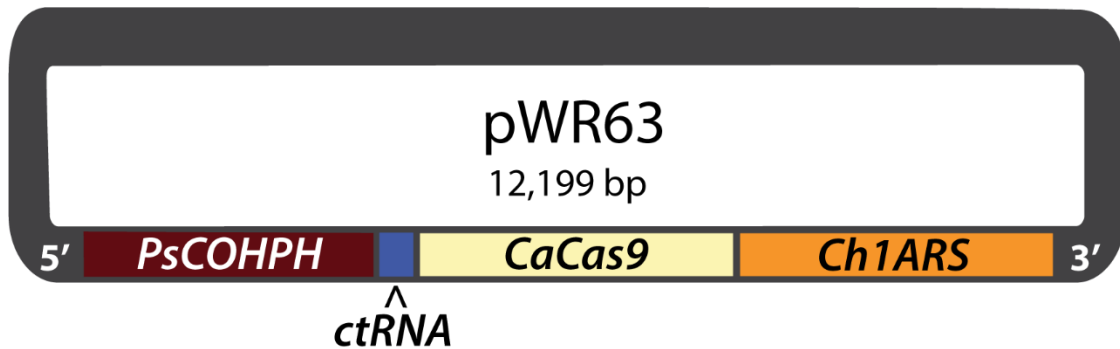


Figure 13, the pWR63(*YUMI*) blink out plasmid. The Chromosome 1, Autonomous Replicating Sequence (*Ch1ARS*) allows the blink out plasmid to replicate as a circular plasmid inside *S. stipitis* once transformed.

After Δ *HXK1* *S. stipitis* was transformed with the circular pWR63(*YUMI*) plasmid, successful transformants lost their ability to bioluminesce yet they gained

conditional resistance to Hygromycin as long as the plasmid remains within the cells. The Cas9 cuts the *YUMI* targets of the integrated BLINCAR element, removing the bioluminescence and Geneticin resistance genes (Figure 14). This cut causes a DSB allowing the Cas9 Actuated Recombination (CAR) regions to recombine using HR machinery. This leaves a single CAR scar where the *HXK1* gene was (Figure 15).

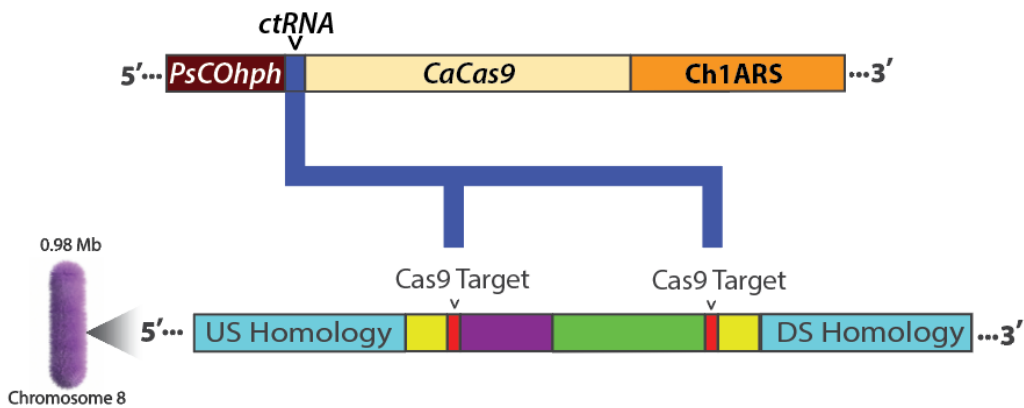


Figure 14, the blink out plasmid encodes a *ctRNA* that guides the Cas9 protein to excise the blink in element at the Cas9 targets.

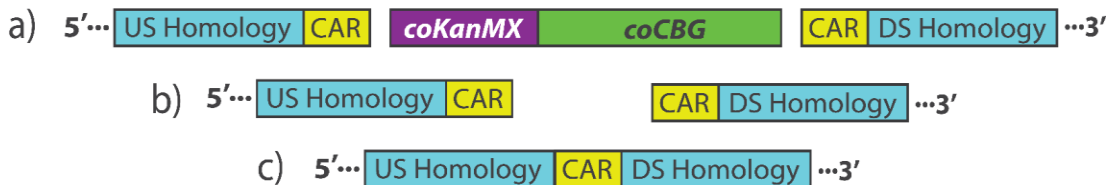


Figure 15, After excision of the blink in element (a-b) containing the *CoKanMX* and *CoCBG-99* genes, the DSB is rejoined via HR leaving a scar at the CAR site (c).

The resultant pWR63(*YUMI*)-transformed colonies were selected on hygromycin. Luciferin was included in the media to identify non-bioluminescent colonies (Figure 16). At least 11 non-glowing colonies were detected. For colonies labeled 1, 2, and 3 genomic DNA was isolated for further testing. To ensure that the BLINCAR element was removed a PCR test was performed on those three candidate strains (Figure 17). Primers were chosen to amplify a region outside of the upstream and downstream homologies (Figure 17 (a)). If the BLINCAR element failed to be removed, the distance between these primers would be approximately 10 kb and likely too large to produce a PCR product. However, if Cas9 was successful at removing the BLINCAR element and the chromosome repaired itself by HR, then the distance between the primers would be 4.6 kb and a more reasonable size to amplify using PCR during the extension time used. Two of the three candidate colonies PCR tested positive (or negative for the blink in element) for the absence of the blink in element (Figure 17 (b)).

I now had a *HXK1* knockout *S. stipitis* yeast strain that was once again sensitive to Geneticin, and after growing the strain in liquid culture from a dilute inoculum without Hygromycin, the pWR63(*YUMI*) plasmid was lost from the strain and the strain thereby regained sensitivity to Hygromycin as well. I then tested this yeast's ability to ferment a mixture of glucose and xylose compared to the wild type.

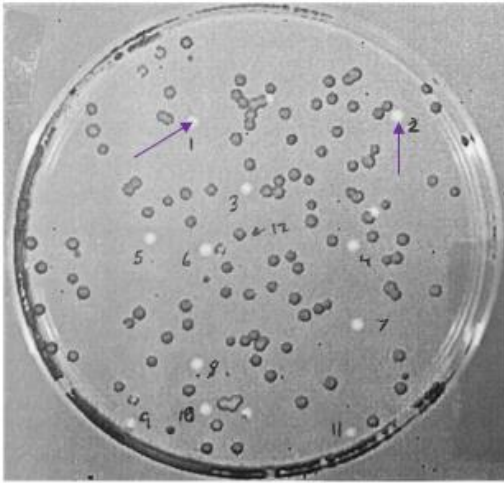
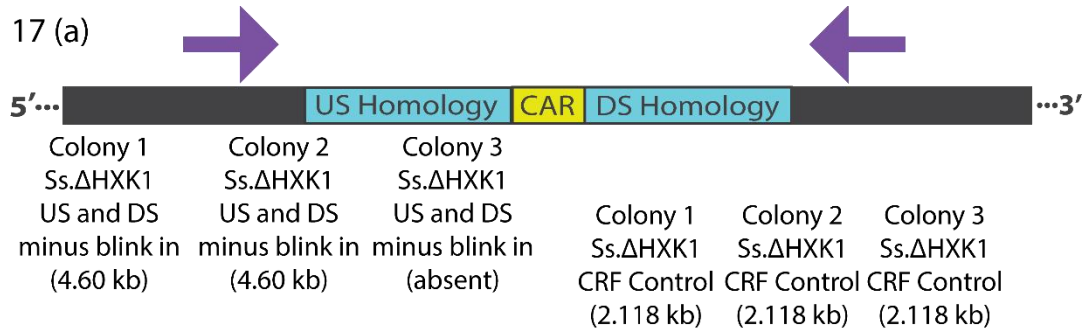


Figure 16, Photograph of the non-bioluminescent colonies (purple arrows) that have been blinked out. The picture consists of merged images comprising a brightfield image showing all colonies and an inverted bioluminescent image (5 minute exposure) with bioluminescence showing up as black colonies. White colonies are the ones not glowing.



17 (b)

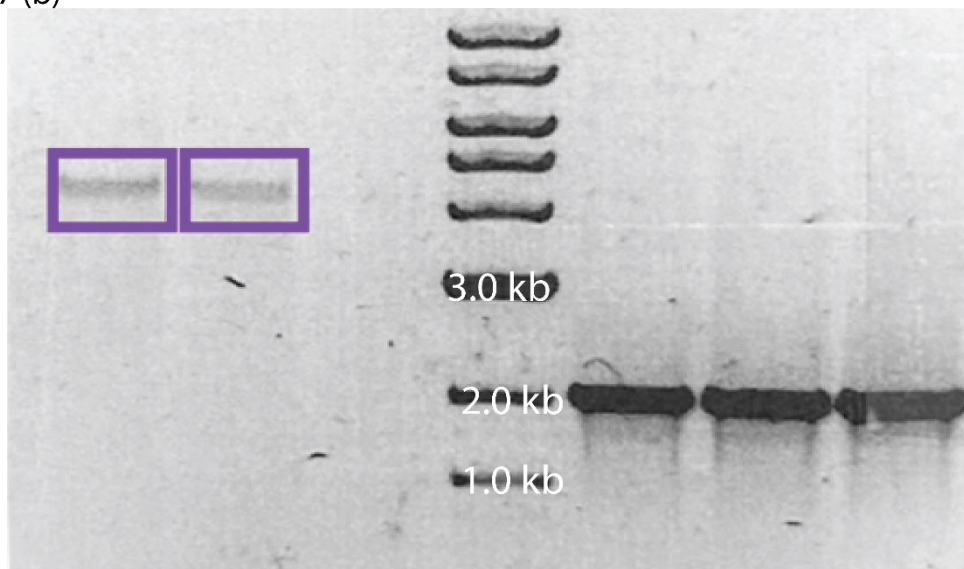


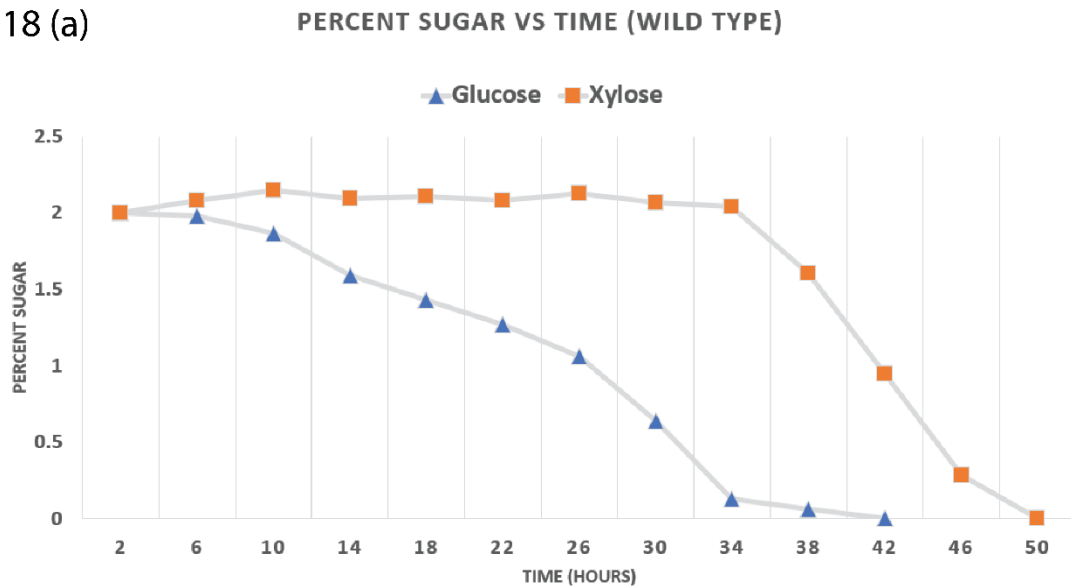
Figure 17 (a) A model illustrating the PCR screen to detect removal of the BLINCAR element. Primers shown as purple arrows amplify a region that includes both US and DS homologies and the CAR scar. The primers amplify a sequence of 4.60kb. **Figure 17 (b) A PCR screen of 3 candidate strains for removal of the BLINCAR element.** Successful removal yields a band at the expected 4.60kb. The purple boxes show these PCR products. Also shown to the right of the ladder is a positive control PCR reaction for each strain's genomic DNA.

Objective (4), Comparing sugar usage of the mutant yeast versus the wild type:

I cultured wild type *S. stipitis* and $\Delta HXK1$ *S. stipitis* on YPX (1% Yeast Extract, 2% Peptone, 2% Xylose) agar plates to establish actively growing cultures. Next, I used hemocytometry to count dilutions of the actively growing yeast and inoculate separate cultures ($\Delta HXK1$ and wild type) using approximately similar numbers of cells of each strain. These inoculations were made in mixed sugar minimal conditions with a final concentration of 4% total sugar per liquid media treatment. In the mixed sugar assay, I used a mixture of 2% glucose and 2% xylose. I recovered supernatant samples every four hours over a 36 hour-period. I measured samples for turbidity and then I centrifuged 500 μ l of sample briefly to pellet the cells. The supernatant was then carefully aliquoted and stored at -80°C in a labelled 1.5 mL microfuge tube for HPLC analysis of sugar content (Figure 18).

The wild type and the $\Delta HXK1$ yeasts exhibit similar properties when grown in mixed sugar media (Figure 18). The control group consists of wild type yeasts which have an in-tact *HXK1*. The mutant strain, however, has *HXK1* removed.

18 (a)



18 (b)

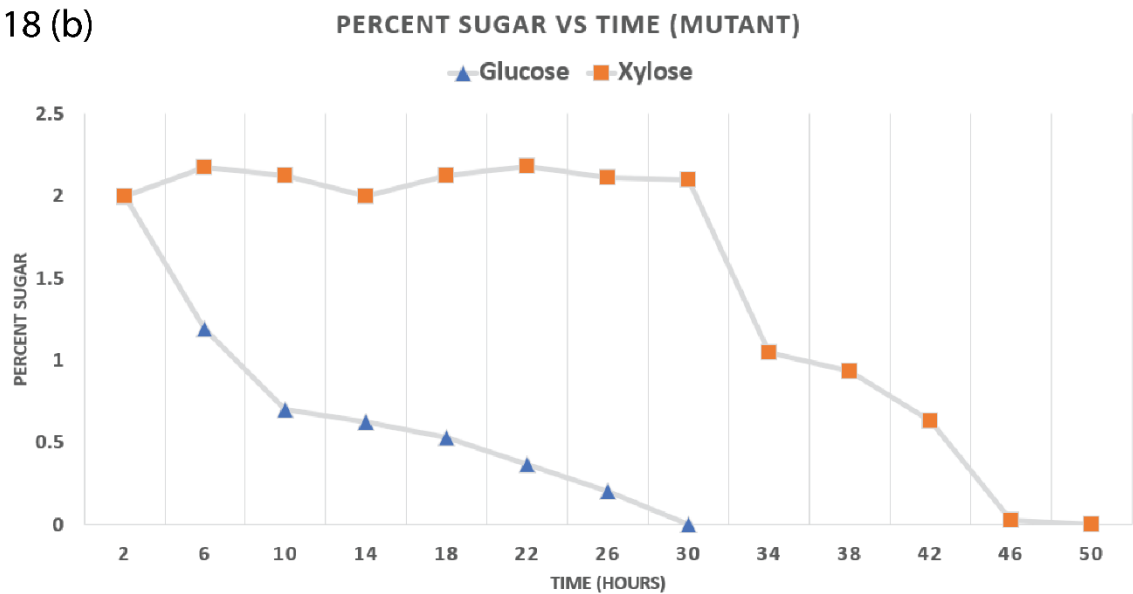


Figure 18, the wild type vs. the mutant *S. stipitis* sugar consumption patterns. Figure 18 (a) shows that for the mutant, the time of glucose expiration coincides with the initiation of xylose fermentation. Figure 18 (b) shows that the wild type, just like the mutant, has a glucose depletion point concomitant with xylose consumption. These are theoretical observations based off of the starting concentration pegged at 2%.

According to the HPLC data results, in figure 18, deleting *HXK1* was not enough to make the mutant strain ferment xylose at the same time as glucose. Xylose is consumed when all the glucose was depleted in both w.t. and mutant strains. This indicates that in the absence of *HXK1*, a redundant hexokinase has stepped up to be the primary glucose phosphorylator. Although the phenotypic traits were not altered, I have successfully modified the genotypic traits. This is enough to demonstrate the utility of the BLINCAR system, however, deleting *HXK1* is not sufficient to induce glucose and xylose cofermentation. This led me to hypothesize that one or more hexokinases must be deleted in order to achieve co-fermentation of glucose and xylose. In order to see which other kinases may be playing a role in phosphorylating glucose, I followed the fermentation experiment up with a qRT-PCR.

In light of my HPLC data, I designed a qRT-PCR experiment to determine which hexokinases contribute to glucose phosphorylation in *S. stipitis*. The hexokinase responsible should be upregulated compared to the other hexokinases when grown on glucose. I grew up mutant and w.t. *S. stipitis* in minimal glucose medium and performed an RNA extraction on both while they were actively growing in log phase. After extracting the RNA product, it was used to make cDNA, the template in our qRT-PCR reactions. My qRT-PCR experiment included primers to amplify two reference mRNAs (*ACT1* and *TAF10*) and each of the known glucose kinase homologs (*HXK1*, *GLK1*, *GLK2*, and *NAG5*).

Table 1, the C_q values reveal that *GLK2* is transcribed 2000x that of other enzymes.

Amplicon	<i>ACT1</i>	<i>TAF10</i>	<i>HXK1</i>	<i>GLK1</i>	<i>GLK2</i>	<i>NAG5</i>
WT C_q Value rep. 1	20.4	18.2	30.7	25.7	17.4	36.9
WT C_q Value rep. 2	20.3	17.7	27.5	26.5	17.5	36.5
WT C_q Value rep. 3	21.0	17.4	29.1	25.1	18.0	-
Mut C_q Value rep. 1	20.6	18.2	-	29.7	18.3	-
Mut C_q Value rep. 2	21.3	19.4	-	28.7	17.7	-
Mut C_q Value rep. 3	20.4	17.2	-	26.6	17.8	33.7
WT C_q Value mean	20.6	17.8	29.1	25.8	17.6	36.7
Mut C_q Value mean	20.8	18.3	-	28.3	17.9	33.7

From the data shown in table 1, it appears that *GLK2*, glucokinase 2, is expressed approximately 2000x that of other hexokinases. This suggests that the protein from *GLK2* is likely doing the bulk of the glucose phosphorylation, regardless of whether *HXK1* was removed or not. Our assumption that *HXK1* was the primary glucose phosphorylator seems to be wrong. It is important to remember that different targets will be amplified with differing efficiency. Furthermore, mRNA and protein levels may not be directly related.

Materials and Methods

Table 2, the table of primers used in this study

No.	Primer Name	Sequence (5'-3')
1	<i>HXK1</i> usB(AgeHind)5	actactACCGGTGAAGCTTCCTGTTCCAGA
2	<i>HXK1</i> us(XbaI)3	tcatcaTCTAGAGTGTAAGTAGTTGGATAAGGTGTC
3	<i>HXK1</i> ds(Nde)5	actactCATATGTCTCTAAGTCAAATGTCCATGT
4	<i>HXK1</i> ds(Sac2Hind)3	actactCCGCGGAAGCTTATGATATCCTTGAATTCGTC
5	<i>HXK1</i> usScrnB5	CTCTTCAGTTCACCCAAATC

6	<i>HXK1</i> dsScrnB3	TGTAGCATCTTGCAAATGAG
7	PsCBGscrn5	AAACAATTGTTGGAGAAGGC
8	PsKanScrn3	CGTGAGTCTTTTCCTTACCC
9	qACT1-5	TTGTTTTGGACTCTGGTGA
10	qACT1-3	GTCAGTCAAGTCTCTACCGG
11	qTAF10-5	TTCTTCAACTGTCACTGCTG
12	qTAF10-3	TATAATGGGAGCAAAGTCG
13	q <i>HXK1</i> -5	TTGTTTGAAGAAGTTTGTGG
14	q <i>HXK1</i> -3	AAGAAACCTTCGTTGATAGAA
15	q <i>GLK1</i> -5	GTCGAATTATTGCAGAAGC
16	q <i>GLK1</i> -3	GTATTGGAATTTGTCTTGGAA
17	q <i>GLK2</i> -5	GGCTAATGTTCGACAAGATG
18	q <i>GLK2</i> -3	TTCTTCAGCTCGTTCAGAC
19	q <i>NAG5</i> -5	TTTGAAGACCACATCGTACA
20	q <i>NAG5</i> -3	TCAATGTGTAATCAAACCTCG

Microbial Strains, Media, and General Culture Conditions

For all *E. coli* transformations, I used TOP10 chemically competent cells for all plasmid production and cloning purposes. The yeast experiments utilized the wild-type *S. stipitis* strain CBS 6054 (ATCC 58785). *Escherichia coli* bacteria were cultivated in either solid or liquid LB (Luria-Bertani) medium (10 g/L Tryptone, 10 g/L NaCl, 5 g/L Yeast extract) supplemented with 100 µg/mL ampicillin. *S. stipitis* was cultivated for a duration of one night at a temperature of 30°C in liquid YPD medium, which consisted of 1% yeast extract, 2% peptone, and 2% dextrose. Additionally, *S. stipitis* was also cultured on solid YPD medium containing 2% agar. Sometimes these media contained one or more of the following additives: 200 µg/mL G-418, 200 µg/mL Hygromycin, 100 µM beetle luciferin sodium salt. For the fermentation experiment, minimal xylose/glucose medium consisted of 0.67% YNB (without amino acids and ammonium sulfate) Yeast

Nitrogen Base, (Becton Dickinson) medium with 2% glucose, 2% xylose, and 0.225 % urea.

Transforming plasmids into bacteria

For all transformations, I thawed a 100 μ L aliquot of TOP10 competent *E. coli* (from a -80°C freezer) on ice for 30 minutes. I mixed 1-5 μ L of plasmid DNA into the culture. After flicking the tube to mix, I incubated the reaction at 4°C for 30 minutes. I heat shocked the cells at 42°C for 45 seconds. I immediately put the tubes back on ice for two minutes to recover. After this, I added 1 mL LB media and outgrew the culture at 37°C in a shaking incubator for 45 minutes. After outgrowth, I pipetted 50 μ L of cells onto an LB agar plate with 100 $\mu\text{g/ml}$ ampicillin. I used sterile 1 mm glass beads to evenly distribute the inoculum. I incubated the plate overnight at 37°C . I PCR-screened colonies to confirm successful transformation.

PCR

I used PCR for two purposes in my work. The first reason was to generate end-modified copies of homology arms for inserting into recombinant vectors. The second reason was to screen candidate colonies for proper genetic modification. I used goTaq (Promega) to carry out all of the PCR reactions. I used primers 1 and 2 (Table 2) to amplify the upstream homology arm (1,768 bp) and used primers 3 and 4 to amplify the downstream (2,118 bp) homology arm for insertion into the pWR95 plasmid. Both 50 μ L reactions had an annealing temperature of 60°C and an extension time of two minutes. I

used the primers 5 and 7 to amplify a 3.2 kb upstream amplicon and primers 6 and 8 to amplify the downstream 3.2kb amplicon. These 50 μ L reactions had an annealing temperature of 60°C and an extension time of 3 minutes and twenty seconds. For all other variables of the PCR reaction, I followed the manufacturer's recommendations.

qRT-PCR

I used qRT-PCR to generate copies of portions of a series of genes found in both the wild type and the mutant *S. stipitis* yeasts. Some of the genes targeted are control groups while the genes which are directly involved in glycolysis (the four hexokinases) are test groups. Primers 9, and 10 and primers 11 and 12 both amplify two maintenance genes (*ACT1* and *TAF10*) that are transcribed into mRNA by both the wild type and the hexokinase mutant. The test groups, primers 13-20, however, amplify portions of the four genes responsible for the hexokinases (*HXK1*, *GLK1*, *GLK2*, *NAG5*). All primer sets in the qRT-PCR experiment had an annealing temperature of 60°C. I used the Verso SYBR Green1Step qRT-PCR kit (# AB-4104A, Thermo Scientific) and manufacturer's recommended reaction mixes and cycle protocol.

Transforming exogenous DNA into *S. stipitis*

I digested 60 μ g of *HXK1*-USDS-pWR95 plasmid DNA with *HindIII* in a 200 μ L reaction, leaving homology on both sides of the deletion cassette. DNA was ethanol precipitated and resuspended in 20 μ L of water. I concentrated 10 mL of log-phase-growing *S. stipitis* cells by centrifugation at 3000 RPM for 5 minutes. I next washed the

cells with 1000 μL TE/LiOAc (1x TE, 0.1 M lithium acetate) and collected cells at 3000 RPM, 5 minutes. Afterwards I washed the cells with 500 μL TE/LiOAc (at 3000 RPM, 5 minutes). I resuspended the cells in 100 μL TE/LiOAc. I added plasmid DNA (either 10 μg of circular plasmid or 60 μg of linearized plasmid) + 30 μL Herring sperm DNA (10 mg/mL, Promega) + 700 μL PEG/TE/LiOAc (1x TE, 0.1 M lithium acetate, 40% polyethylene glycol-8000). I incubated the mixture at 30°C on roller for 30 minutes. Next, I heat shocked the cells for 5 minutes at 42°C. I spun the cells around 8 seconds at 4000-6000 RPM and I removed the supernatant. For antibiotic selection, I resuspended the cells in 3 mL YPD and outgrew them for 4 hours then plated them on YPD or YPX plates containing the appropriate antibiotic (hygromycin or G-418). This protocol is rooted in the works of Ito, *et al*, 1983 and a protocol published at the Dunham lab at the University of Washington in which they transform *S. cerevisiae* (Dunham, 2004) but was refined for *S. stipitis* by the Robertson Lab (Reichard *et al.*, 2023).

Agarose Gel Electrophoresis

I used gel electrophoresis for primarily two reasons. The first is to determine the sizes of linearized DNA and second to size-select and excise particular DNA fragments for use in recombinant plasmid construction. I used TAE as a buffer and all gels consisted of 1% agarose (SeaKem Gold Agarose). I included SYBR Safe DNA stain (0.1 $\mu\text{L}/\text{mL}$) (Thermo Fisher). When gel extraction was needed, I used a GeneJet gel extraction kit (Thermo Fisher).

Yeast RNA Isolation

I cultured the *S. stipitis* cells overnight in YNB + Glucose (2%) + Urea (0.225 %) at 30°C in a shaking incubator. I made a 1/5 dilution in a 10 mL culture and grew it in the same medium and conditions for 4 hours (This step was meant to get the culture actively growing and metabolizing the sugar). I chilled the cells on ice. I then collected 1 mL samples in microcentrifuge tubes and centrifuged at 17,000 g for 1 minute at 4°C to pellet cells. Afterwards, I resuspended the pellets in 200 µL cold LME buffer (100 mM LiCl, 100 mM MOPS, 1 mM EDTA) and added 1% SDS and 2% Triton-X100. I next added 300 µL 1 mm glass beads and 200 µL of cold Phenol/Chloroform/Isoamyl Alcohol (25:24:1). I vortexed microfuge tubes for 30 seconds followed by 30 seconds on ice to lyse cells. I Repeated the vortex and ice cycle for total of 4 treatments (2 minutes total vortex). After lysis cycles, I added 200 µL cold LME buffer and vortexed for 10 seconds to mix. I centrifuged the sample at 17,000 g for 5 minutes at 4°C to separate the phases. I moved the top (aqueous) phase (about 350 µL) to a new microcentrifuge tube. After discarding the phenol and beads into the proper hazardous waste receptacle I added to the aqueous phase 50 µL of cold LME and 400 µL of cold Phenol/Chloroform/Isoamyl Alcohol (25:24:1) for a second extraction. I vortexed for 30 seconds and centrifuged as before to separate the layers. Next, I moved the top (aqueous) phase to a new microcentrifuge tube. This volume again is about 350 µL. To the aqueous phase, I added 50 µL of cold LME and 400 µL of cold Phenol/Chloroform/Isoamyl Alcohol (25:24:1) for a third extraction. Vortex for 30 seconds and centrifuge as before to separate layers. I then move the top (aqueous) phase to a new microcentrifuge tube.

To the aqueous phase, I added 400 μ L of chloroform. I vortexed for 30 seconds and centrifuged as before to separate layers. I moved the top (aqueous) phase to a new microcentrifuge tube (around 300 μ L). I added 1/10 of the volume of 3 M Sodium Acetate (DEPC treated) and 2 volumes of cold 100% EtOH. I vortexed briefly to mix and store overnight at -20°C so that RNA could precipitate. The next day, I centrifuged at 17,000 g for 20 min at 4°C. I emptied the supernatant and added cold 80% EtOH (made with nuclease-free water) to the pellet to wash. I centrifuged at 17,000 g for 15 minutes at 4°C. Afterwards, I used a vacuum aspirator with a clean tip to remove the supernatant. I let the RNA pellet dry in a fume hood for 15 minutes. Finally, I resuspended the pellet in 25 μ L of nuclease-free water.

Bioluminescent and Brightfield Image Acquisition

Yeast that was grown on solid medium in 10 cm Petri plates was imaged using a ChemiDoc MP (Bio-Rad, Hercules, CA). The imaging was done in both bioluminescent and brightfield modes. The bioluminescent images were captured with a 4 x 4 binning with exposure periods ranging from 1 to 5 minutes.

Mixed Sugar Fermentation Conditions and HPLC Analysis

HXK1 knockout and wild type yeasts were fermented in mixed sugar media conditions. The minimal liquid medium for the fermentation experiment was made of 6.7 g/L YNB, 2% Glucose, 2% Xylose, and 0.225% urea. After cells reach confluency, they were washed twice with ice cold water. After this they were adequately diluted (based off

of their absorbance) in minimal media to ensure that the mutant and wild type both begin fermenting with the same concentration of cells. This volume of cells was resuspended with cold YNB 2% Glucose, 2% Xylose, and 0.225% urea. This cell-media mixture was supplemented by the final volume of the fermentation vessel. The cells were pipetted into the fermentation vessel. Initial samples were taken at $t = 0$. Samples were fermented in a shaking incubator at 200 RPM at 30°C. After this first sample, I took 500 μL samples every four hours over a 36-hour period. Every time samples were recovered, they were centrifuged and the supernatant was preserved for later HPLC analysis in a -80°C freezer.

The purpose of the HPLC analysis is to determine the concentrations of both sugars at any time point during the fermentation. A Dionex 3000 HPLC system equipped with a RefractoMax 520 refractive index detector was used to analyze samples. Chromatography was carried out using a Bio-Rad Aminex HPX-87H (7.8 mm x 300 mm; 9 μm) column. The mobile phase was HPLC grade water at a flow rate of 0.30 mL/minute. The column temperature was 40°C and 10 μL of sample was injected.

Restriction Digestion of DNA

I used restriction digestion for three purposes. The first purpose was to create DNA fragments with appropriate sticky ends for plasmid construction, in which case the amount of DNA used in those reactions was approximately 1 to 2 μg in 20 μL reactions. The second reason I used restriction digestion was for restriction analysis to confirm proper construction, in which case the amount of DNA was 0.5 to 1 μg in 20 μL reactions. The third reason was to linearize the *HXK1*-USDS-pWR95 plasmid prior to transformation into *S. stipitis*, which used 60 μg in a 200 μL reaction.

Ligation of DNA

Ligation of DNA to other complimentary sticky ends was done with a T4 DNA ligase (New England Biolabs). A ligation reaction consisted of vector DNA, insert DNA in a 1:3 molar ratio of vector to insert buffer, water, and T4 DNA ligase enzyme. All components were mixed into a 20 μ L reaction and from this were incubated at 4°C for 24-36 hours.

Conclusion

This project revolved around engineering a *S. stipitis* yeast that favors xylose over glucose when compared to the wild type. The goal was to engineer a xylose auxotroph to more efficiently convert xylose into ethanol. This would result in a yeast that ferments xylose and glucose at the same time. To reach this end, I used the BLINCAR system to knock out the first enzyme involved in glycolysis, *HXK1*. This entailed replacing the *HXK1* gene with a bioluminescent reporter element, followed by removing the element using a Cas9 nuclease. I used bioluminescence and PCR assays to verify that I removed then replaced the *HXK1* gene. I set out to first demonstrate the utility of the BLINCAR system and secondly to test a mutant phenotype versus a wild type phenotype.

It was hypothesized that removing *HXK1* from *S. stipitis* would result in the organism's metabolism shifting away from glucose and toward xylose when it was cultivated on a mixed sugar. The BLINCAR system was able to successfully knock out *HXK1*, but I did not see any differences in the manner that wild-type yeast metabolizes

glucose in comparison to the mutant. Because of this, it may be deduced that if *HXK1* is not present, a different hexokinase will take over as the principal glucose phosphorylator. I discovered that glucokinase 2, a hexokinase homologue, is likely responsible for glucose phosphorylation by carrying out a qRT-PCR test.

It seems that my hypothesis is not supported by the data. I was surprised not to see a difference in glucose metabolism as noted in the paper written by Dashtban *et al* 2015. The future for this project would involve knocking out *GLK2* and testing the mutant's mixed sugar fermentation compared to the wild type.

The identity of *HXK1* may be lost in translation – meaning that it was mislabeled. We based our assumption from a paper written by Jeffries *et al* before there were clear analogues or descriptions from the genome sequencing (Jeffries *et al* 2009). Sometimes proteins are mislabeled and then relabeled after phylogenetic analysis. Because *GLK2* is produced in such high amounts we conclude that it is the primary glucose phosphorylator, which may mean that the protein should be reclassified as *HXK1*. We also based our choice off *HXK1*, however, in *S. cerevisiae*, *HXK2* is the primary glucose phosphorylator (Herrero *et al* 1995). *HXK1* was named based on sequence similarity to orthologues *S. cerevisiae*, not necessarily their roles. Besides focusing on a different gene (*GLK2*) there are many other avenues that this project could take.

Instead of knocking out the hexokinase genes, I could knock out the genes that encode for membrane bound glucose transport. When this was done in *S. cerevisiae*, it resulted in a yeast that is incapable of consuming any glucose (Reifenberger *et al* 1997). In another publication, a *S. cerevisiae* yeast was fitted with *S. stipitis* xylose transmembrane transport machinery so that it was forced to consume only xylose

(Weierstall *et al* 1990). There are some transmembrane hexose transporters that can transport both glucose and xylose (Farwick *et al*, 2014). A study directed on knocking out the glucose transporters in *S. stipitis* would involve introducing genetic elements that remove or truncate their respective glucose transport genes. This, however, might not work because the receptors have higher affinity for glucose.

Another approach, besides molecularly altering the yeast, is using a different yeast altogether. *S. stipitis* is not the best yeast for biofuels. Another beetle gut symbiote, *Spathospora passalidarum*, has recently demonstrated a much higher fermentative capacity compared to *S. stipitis* (Selim *et al* 2020). *S. passalidarum* accumulates 1.5 times more ethanol than *S. stipitis* in oxygen limited conditions (Veras *et al* 2017). It stands to reason that the yeast, like *S. stipitis*, can be engineered to be even better at converting xylose into ethanol.

Yeast biofuels may not be the most efficient or economically feasible option for parties interested in renewable energy. Another consideration is the low alcohol percentage produced by *S. stipitis*. The alcohol content has not been recorded to be above 4% for the xylose fermenting yeasts (Campos *et al* 2022). Another project could be to build a more ethanol tolerant yeast.

Cellulosic ethanol has problems. There is not much biomass available. Pretreatment using acids or hydrolysis generates toxins. Finally, yeasts are sensitive to acetic acid regardless of which sugars they can or cannot process.

In conclusion, the development and engineering of a *S. stipitis* yeast strain capable of simultaneous glucose and xylose utilization represent a significant advancement in biotechnology with vast implications for various industries, particularly biofuel production. Through meticulous experimentation and genetic manipulation, this thesis has demonstrated the feasibility and potential of such a strain, highlighting the importance of metabolic engineering in addressing challenges associated with renewable energy sources. The successful creation of this dual-utilizing yeast would not only contribute to the optimization of bioethanol production processes but also underscores the broader potential for innovative solutions in sustainable bioprocessing. As we continue to explore and refine the capabilities of microbial organisms, the findings presented herein offer valuable insights into the intricate mechanisms of cellular metabolism and pave the way for further advancements in the field of biotechnology.

References

Badr, C. E., and Tannous, B. A. (2011). Bioluminescence imaging: progress and applications. In *Trends in Biotechnology* (Vol. 29, Issue 12, pp. 624–633). Elsevier BV.

<https://doi.org/10.1016/j.tibtech.2011.06.010>

Baldwin, T. O. (1996). Firefly luciferase: the structure is known, but the mystery remains. In *Structure* (Vol. 4, Issue 3, pp. 223–228). Elsevier BV.

[https://doi.org/10.1016/s0969-2126\(96\)00026-3](https://doi.org/10.1016/s0969-2126(96)00026-3)

Barcelos, M. C. S., Lupki, F. B., Campolina, G. A., Nelson, D. L., and Molina, G. (2018). The colors of biotechnology: general overview and developments of white, green and blue areas. In *FEMS Microbiology Letters* (Vol. 365, Issue 21). Oxford University Press

(OUP). <https://doi.org/10.1093/femsle/fny239>

Branchini, B. R., Fontaine, D. M., Kohrt, D., Huta, B. P., Racela, A. R., Fort, B. R., Southworth, T. L., and Roda, A. (2022). Systematic Comparison of Beetle Luciferase-Luciferin Pairs as Sources of Near-Infrared Light for In Vitro and In Vivo Applications. In *International Journal of Molecular Sciences* (Vol. 23, Issue 5, p. 2451). MDPI AG.

<https://doi.org/10.3390/ijms23052451>

Campos, V. J., Ribeiro, L. E., Albuini, F. M., de Castro, A. G., Fontes, P. P., da Silveira, W. B., Rosa, C. A., and Fietto, L. G. (2022). Physiological comparisons among *Spathaspora passalidarum*, *Spathaspora arborariae*, and *Scheffersomyces stipitis* reveal the bottlenecks for their use in the production of second-generation ethanol. In *Brazilian Journal of Microbiology* (Vol. 53, Issue 2, pp. 977–990). Springer Science and Business Media LLC. <https://doi.org/10.1007/s42770-022-00693-6>

Charles, M. B., Ryan, R., Ryan, N., and Oloruntoba, R. (2007). Public policy and biofuels: The way forward? In *Energy Policy* (Vol. 35, Issue 11, pp. 5737–5746). Elsevier BV. <https://doi.org/10.1016/j.enpol.2007.06.008>

Chylinski, K., Makarova, K. S., Charpentier, E., and Koonin, E. V. (2014). Classification and evolution of type II CRISPR-Cas systems. In *Nucleic Acids Research* (Vol. 42, Issue 10, pp. 6091–6105). Oxford University Press (OUP). <https://doi.org/10.1093/nar/gku241>

Constantinou, A., Davies, A. A., and West, S. C. (2001). Branch Migration and Holliday Junction Resolution Catalyzed by Activities from Mammalian Cells. In *Cell* (Vol. 104, Issue 2, pp. 259–268). Elsevier BV. [https://doi.org/10.1016/s0092-8674\(01\)00210-0](https://doi.org/10.1016/s0092-8674(01)00210-0)

Cruz, Carlos H. Brito, Glaucia Mendes Souza and Luiz A. Barbosa Cortez. (2014). Biofuels for Transport. In *Future Energy Second Edition* (pp. 8-9). Elsevier.

Dashtban, M., Wen, X., Bajwa, P. K., Ho, C.-Y., and Lee, H. (2015). Deletion of *HXXI* gene results in derepression of xylose utilization in *Scheffersomyces stipitis*. In *Journal of Industrial Microbiology and Biotechnology* (Vol. 42, Issue 6, pp. 889–896). Oxford University Press (OUP). <https://doi.org/10.1007/s10295-015-1614-9>

Day, J. C., Tisi, L. C., and Bailey, M. J. (2004). Evolution of beetle bioluminescence: the origin of beetle luciferin. In *Luminescence* (Vol. 19, Issue 1, pp. 8–20). Wiley. <https://doi.org/10.1002/bio.749>

Fan, F., and Wood, K. V. (2007). Bioluminescent Assays for High-Throughput Screening. In *Assay and Drug Development Technologies* (Vol. 5, Issue 1, pp. 127–136). Mary Ann Liebert Inc. <https://doi.org/10.1089/adt.2006.053>

Farwick, A., Bruder, S., Schadeweg, V., Oreb, M., and Boles, E. (2014). Engineering of yeast hexose transporters to transport delta-xylose without inhibition by delta-glucose. In *Proceedings of the National Academy of Sciences* (Vol. 111, Issue 14, pp. 5159–5164). *Proceedings of the National Academy of Sciences*. <https://doi.org/10.1073/pnas.1323464111>

Fleiss, A., and Sarkisyan, K. S. (2019). A brief review of bioluminescent systems (2019). In *Current Genetics* (Vol. 65, Issue 4, pp. 877–882). Springer Science and Business Media LLC. <https://doi.org/10.1007/s00294-019-00951-5>

Gandam, P. K., Chinta, M. L., Gandham, A. P., Pabbathi, N. P. P., Konakanchi, S., Bhavanam, A., Atchuta, S. R., Baadhe, R. R., and Bhatia, R. K. (2022). A New Insight into the Composition and Physical Characteristics of Corncob—Substantiating Its Potential for Tailored Biorefinery Objectives. In *Fermentation* (Vol. 8, Issue 12, p. 704). MDPI AG. <https://doi.org/10.3390/fermentation8120704>

Gao, M., Cao, M., Suástegui, M., Walker, J., Rodriguez Quiroz, N., Wu, Y., Tribby, D., Okerlund, A., Stanley, L., Shanks, J. V., and Shao, Z. (2016). Innovating a Nonconventional Yeast Platform for Producing Shikimate as the Building Block of High-Value Aromatics. In *ACS Synthetic Biology* (Vol. 6, Issue 1, pp. 29–38). American Chemical Society (ACS). <https://doi.org/10.1021/acssynbio.6b00132>

Harvey, E. N., and Stevens, K. P. (1928). The brightness of the light of the West Indian Elaterid beetle, *Pyrophorus*. In *Journal of General Physiology* (Vol. 12, Issue 2, pp. 269–272). Rockefeller University Press. <https://doi.org/10.1085/jgp.12.2.269>

Hastings, J. W. (1983). Biological diversity, chemical mechanisms, and the evolutionary origins of bioluminescent systems. In *Journal of Molecular Evolution* (Vol. 19, Issue 5, pp. 309–321). Springer Science and Business Media LLC. <https://doi.org/10.1007/bf02101634>

Herrero, P., Galíndez, J., Ruiz, N., Martínez-Campa, C., & Moreno, F. (1995).

Transcriptional regulation of the *Saccharomyces cerevisiae* *HXK1*, *HXK2* and *GLK1* genes. In *Yeast* (Vol. 11, Issue 2, pp. 137–144). Wiley.

<https://doi.org/10.1002/yea.320110205>

Ito, H., Fukuda, Y., Murata, K., and Kimura, A. (1983). Transformation of intact yeast cells treated with alkali cations. In *Journal of Bacteriology* (Vol. 153, Issue 1, pp. 163–

168). American Society for Microbiology. <https://doi.org/10.1128/jb.153.1.163-168.1983>

Jeffries, T. W., & Van Vleet, J. R. H. (2009). *Pichia stipitis* genomics, transcriptomics, and gene clusters. In *FEMS Yeast Research* (Vol. 9, Issue 6, pp. 793–807). Oxford

University Press (OUP). <https://doi.org/10.1111/j.1567-1364.2009.00525.x>

Jeppsson, M., Bengtsson, O., Franke, K., Lee, H., Hahn-Hägerdal, B., and Gorwa-

Grauslund, M. F. (2006). The expression of a *Pichia stipitis* xylose reductase mutant with higher *K_M* for NADPH increases ethanol production from xylose in recombinant

Saccharomyces cerevisiae. In *Biotechnology and Bioengineering* (Vol. 93, Issue 4, pp. 665–673). Wiley. <https://doi.org/10.1002/bit.20737>

Jinek, M., Chylinski, K., Fonfara, I., Hauer, M., Doudna, J. A., and Charpentier, E.

(2012). A Programmable Dual-RNA–Guided DNA Endonuclease in Adaptive Bacterial Immunity. In *Science* (Vol. 337, Issue 6096, pp. 816–821). American Association for the

Advancement of Science (AAAS). <https://doi.org/10.1126/science.1225829>

Kobayashi, Y., Inokuma, K., Matsuda, M., Kondo, A., and Hasunuma, T. (2021). Resveratrol production from several types of saccharide sources by a recombinant *Scheffersomyces stipitis* strain. In *Metabolic Engineering Communications* (Vol. 13, p. e00188). Elsevier BV. <https://doi.org/10.1016/j.mec.2021.e00188>

Kowalski, Z., Kulczycka, J., Verhé, R., Desender, L., De Clercq, G., Makara, A., Generowicz, N., and Harazin, P. (2022). Second-generation biofuel production from the organic fraction of municipal solid waste. In *Frontiers in Energy Research* (Vol. 10). Frontiers Media SA. <https://doi.org/10.3389/fenrg.2022.919415>

Krejci, L., Altmannova, V., Spirek, M., and Zhao, X. (2012). Homologous recombination and its regulation. In *Nucleic Acids Research* (Vol. 40, Issue 13, pp. 5795–5818). Oxford University Press (OUP). <https://doi.org/10.1093/nar/gks270>

Lee, R. A., and Lavoie, J.-M. (2013). From first- to third-generation biofuels: Challenges of producing a commodity from a biomass of increasing complexity. In *Animal Frontiers* (Vol. 3, Issue 2, pp. 6–11). Oxford University Press (OUP).

<https://doi.org/10.2527/af.2013-0010>

Levy, Hazel. "University of Florida Book of Insects". University of Florida. Archived from the original on 21 December 2008. Retrieved 2 May 2018.

Li, X., and Heyer, W.-D. (2008). Homologous recombination in DNA repair and DNA damage tolerance. In *Cell Research* (Vol. 18, Issue 1, pp. 99–113). Springer Science and Business Media LLC. <https://doi.org/10.1038/cr.2008.1>

Makarova, K. S., and Koonin, E. V. (2015). Annotation and Classification of CRISPR-Cas Systems. In *Methods in Molecular Biology* (pp. 47–75). Springer New York. https://doi.org/10.1007/978-1-4939-2687-9_4

Mengstie, M. A., and Wondimu, B. Z. (2021). Mechanism and Applications of CRISPR/Cas-9-Mediated Genome Editing. In *Biologics: Targets and Therapy: Vol. Volume 15* (pp. 353–361). Informa UK Limited. <https://doi.org/10.2147/btt.s326422>

Mezzanotte, L., Que, I., Kaijzel, E., Branchini, B., Roda, A., and Löwik, C. (2011). Sensitive Dual Color In Vivo Bioluminescence Imaging Using a New Red Codon Optimized Firefly Luciferase and a Green Click Beetle Luciferase. In A. Herrera-Estrella (Ed.), *PLoS ONE* (Vol. 6, Issue 4, p. e19277). Public Library of Science (PLoS). <https://doi.org/10.1371/journal.pone.0019277>

Miloud, T., Henrich, C., and Hämmerling, G. J. (2007). Quantitative comparison of click beetle and firefly luciferases for in vivo bioluminescence imaging. In *Journal of Biomedical Optics* (Vol. 12, Issue 5, p. 054018). SPIE-Intl Soc Optical Eng. <https://doi.org/10.1117/1.2800386>

Morey, Samuel 1826, Morey's Explosive Engine, American Journal of Science and Arts, 11, p. 104

Qiu, M., Liu, R., Li, X., Du, L., Ruan, Q., Pollard, A. M., Zhang, S., Yuan, X., Liu, F., Li, G., Li, G., Jiao, Z., Luo, J., Chen, S., Yang, X., Wang, Y., Han, J., Chen, F., and Dong, G. (2023). Earliest systematic coal exploitation for fuel extended to ~3600 B.P. In Science Advances (Vol. 9, Issue 30). American Association for the Advancement of Science (AAAS). <https://doi.org/10.1126/sciadv.adh0549>

Reichard, W. D., Smith, S. E., and Robertson, J. B. (2023). BLINCAR: a reusable bioluminescent and Cas9-based genetic toolset for repeatedly modifying wild-type *Scheffersomyces stipitis*. In A. P. Mitchell (Ed.), mSphere (Vol. 8, Issue 4). American Society for Microbiology. <https://doi.org/10.1128/msphere.00224-23>

Reifenberger, E., Boles, E., and Ciriacy, M. (1997). Kinetic Characterization of Individual Hexose Transporters of *Saccharomyces cerevisiae* and their Relation to the Triggering Mechanisms of Glucose Repression. In European Journal of Biochemistry (Vol. 245, Issue 2, pp. 324–333). Wiley. <https://doi.org/10.1111/j.1432-1033.1997.00324.x>

Ruchala, J., and Sibirny, A. A. (2020). Pentose metabolism and conversion to biofuels and high-value chemicals in yeasts. In FEMS Microbiology Reviews (Vol. 45, Issue 4). Oxford University Press (OUP). <https://doi.org/10.1093/femsre/fuaa069>

Selim, K. A., Easa, S. M., and El-Diwany, A. I. (2020). The Xylose Metabolizing Yeast *Spathaspora passalidarum* is a Promising Genetic Treasure for Improving Bioethanol Production. In *Fermentation* (Vol. 6, Issue 1, p. 33). MDPI AG.

<https://doi.org/10.3390/fermentation6010033>

Suh, S.-O., McHugh, J. V., Pollock, D. D., and Blackwell, M. (2005). The beetle gut: a hyperdiverse source of novel yeasts. In *Mycological Research* (Vol. 109, Issue 3, pp. 261–265). Elsevier BV. <https://doi.org/10.1017/s0953756205002388>

Thacker, J. (n.d.). Homologous Recombination Repair. In *Encyclopedia of Cancer* (pp. 1410–1413). Springer Berlin Heidelberg. https://doi.org/10.1007/978-3-540-47648-1_2801

United States Environmental Protection Agency. March 22, 2023. Economics of Biofuels. Retrieved from <https://www.epa.gov/environmental-economics/economics-biofuels#:~:text=Replacing%20fossil%20fuels%20with%20biofuels,dependence%20on%20unstable%20foreign%20suppliers.>

U.S. Department of Agriculture. 2022. Feed Grains Sector at a Glance. Retrieved from <https://www.ers.usda.gov/topics/crops/corn-and-other-feed-grains/feed-grains-sector-at-a-glance/>

U.S. Energy Information Administration. July 19, 2022. Biofuels explained. Retrieved from

[https://www.eia.gov/energyexplained/biofuels/#:~:text=Ethanol%E2%80%94an%20alcohol%20fuel%20that,consumption%20\(82%25\)%20in%202021.](https://www.eia.gov/energyexplained/biofuels/#:~:text=Ethanol%E2%80%94an%20alcohol%20fuel%20that,consumption%20(82%25)%20in%202021.)

Veras, H. C. T., Parachin, N. S., and Almeida, J. R. M. (2017). Comparative assessment of fermentative capacity of different xylose-consuming yeasts. In *Microbial Cell Factories* (Vol. 16, Issue 1). Springer Science and Business Media LLC.

<https://doi.org/10.1186/s12934-017-0766-x>

Vyas, V. K., Barrasa, M. I., and Fink, G. R. (2015). A *Candida albicans* CRISPR system permits genetic engineering of essential genes and gene families. In *Science Advances* (Vol. 1, Issue 3). American Association for the Advancement of Science (AAAS).

<https://doi.org/10.1126/sciadv.1500248>

Weierstall, T., Hollenberg, C. P., and Boles, E. (1999). Cloning and characterization of three genes (SUT1-3) encoding glucose transporters of the yeast *Pichia stipitis*. In *Molecular Microbiology* (Vol. 31, Issue 3, pp. 871–883). Wiley.

<https://doi.org/10.1046/j.1365-2958.1999.01224.x>

Yeh, H.-W., and Ai, H.-W. (2019). Development and Applications of Bioluminescent and Chemiluminescent Reporters and Biosensors. In *Annual Review of Analytical*

Chemistry (Vol. 12, Issue 1, pp. 129–150). Annual Reviews.

<https://doi.org/10.1146/annurev-anchem-061318-115027>